EFFECT OF A SUDDEN LEVEL FLUCTUATION ON HOOK FORMATION DURING CONTINUOUS CASTING OF ULTRA-LOW CARBON STEEL SLABS

Joydeep Sengupta and Brian G. Thomas

University of Illinois at Urbana-Champaign,
Department of Mechanical and Industrial Engineering,
1206 West Green Street, Urbana, Illinois USA, 61801

Keywords: Continuous casting, Mold oscillation, Oscillation marks, Hook, Ultra-low carbon steel, Negative strip, Hook formation mechanism, Meniscus

Abstract

Initial solidification in the meniscus region during continuous casting of steel slabs forms periodic surface depressions called oscillation marks, which are often accompanied by sub-surface microstructural features called "hooks". To understand their formation mechanism, a transient finite-element model, CON2D has been applied to compute temperature, stress, and distortion of a steel shell during the initial stages of solidification of ultra-low carbon steel. Furthermore, the effects of sudden metal level fluctuations are investigated. The model uses a creep-type elastic-viscoplastic constitutive equation for steel, which is integrated using a two-level algorithm alternating between solutions at the local node point and the global system of equations. Results show that thermal stress causes the exposed portion of the thin shell to bend away from the mold as the liquid level suddenly drops. The subsequent rise in liquid level increases the bending. The maximum distortion of the shell was found to be ~0.46 mm for a large level drop of 16 mm for 0.4 s. If the deformed shell tip develops enough strength to resist being pushed back to the mold, it will remain embedded in the solidified steel as a hook after the meniscus overflows the deformed shell tip. Further solidification in the overflowed region then creates an oscillation mark.

Introduction

Initial solidification in the mold cavity in a continuous casting machine depends on many complex, coupled phenomena, including local heat transfer, fluid flow, thermal stress, and pressure force fluctuations near the liquid steel meniscus caused by the oscillating mold. As a result, large, irregular transverse depressions and periodic oscillation marks routinely appear on the cast slab surface. Oscillation marks are often accompanied by sub-surface hooks, which often entrap argon bubbles and slag inclusions [1]. To remove these defects, the slab surface typically requires "scarfing" *i.e.* removal of several millimeters of the surface layers which compromises process productivity and yield [2]. This problem particularly plagues steels with low (< 0.1%) carbon contents [3], which makes them difficult to observe [4] .

Figure 1 shows typical shapes and sizes of oscillation marks (OM) and hooks observed on specially-etched samples obtained from ultra-low (0.003% C) carbon steel slabs cast at POSCO

Gwangyang Works, South Korea [2, 4-6]. Hooks can be classified as "curved" (Figure 1(a)) if they angle steeply inwards from the surface or "straight" (Figure 1(b)) if they are shallow and lie just beneath and parallel to the surface [7]. Curved hooks reach deeper beneath the surface (1.42 mm *vs.* 0.48mm for straight hooks) and are accompanied by deeper oscillation marks (0.26 mm *vs.* 0.19 mm for straight hooks). Each hook has a central line, the "line of hook origin", which distinguishes the region inside the hook microstructure from the portion that solidified after liquid steel overflow.
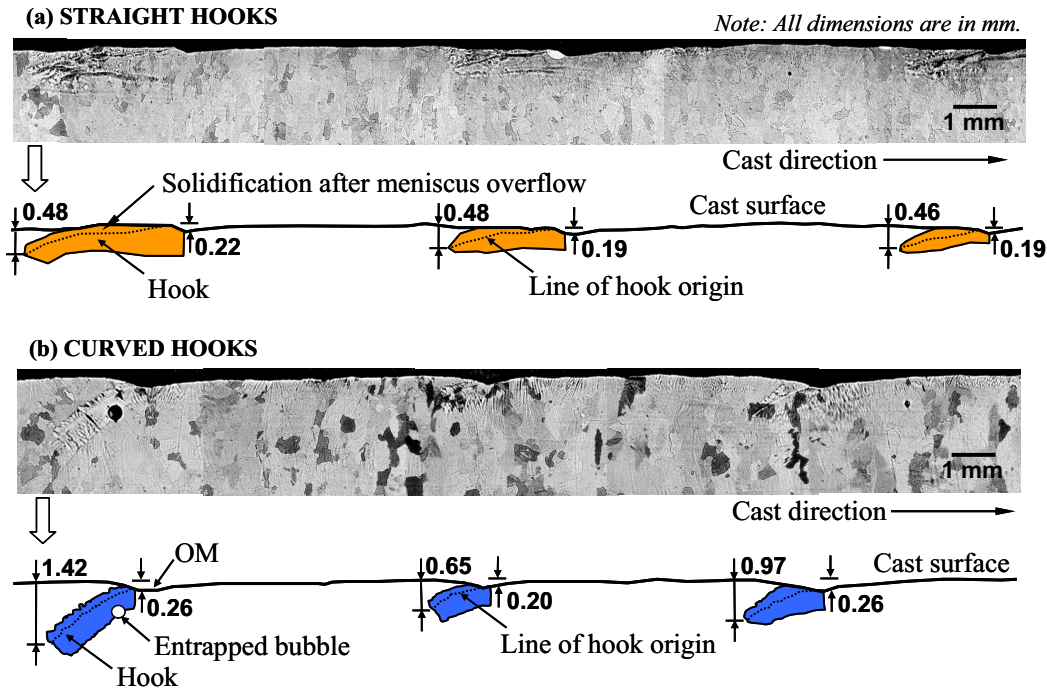

Figure 1: Three consecutive oscillation marks accompanied by (a) curved and (b) straight hooks observed on micrographs obtained from POSCO-cast ultra-low carbon steel slabs [8].

Although oscillation marks, subsurface hooks, and other surface defects have received much attention by past researchers, the mechanism of their formation is yet to be fully understood. Conflicting theories claim that hooks form by (i) bending of the initial shell tip [9, 10], or (ii) freezing of the liquid steel meniscus [11-13]. Similarly, different mechanisms for oscillation marks and surface depressions include: (i) healing of disjointed steel shell edges [14-16], and (ii) mechanical interaction between the mold and shell [17]; (iii) shell bending [9, 10], and (iv) thermal distortion [18] followed by liquid overflow over the shell tip and subsequent solidification. The formation of straight hooks is even less understood.

Very few mathematical models have been applied to understand initial solidification phenomena in the mold cavity to investigate surface defect formation. This is likely due to the difficulty of developing fully-coupled, fully-transient thermal, stress and fluid flow models, which are needed to understand these phenomena. Towards this goal, this study describes the application of a transient thermo-mechanical model to compute temperature, stress development, and distortion of a steel shell during the initial stages of solidification by considering the effect of sudden metal level fluctuations at the meniscus. The model is based on a well-validated transient thermal-elastic-viscoplastic finite element (FE) code, CON2D [19], available at University of Illinois at Urbana-Champaign, and builds on previous work by Thomas and Zhu [18].

Model Description

The model simulates the thermo-mechanical behavior of a solidifying ultra-low carbon steel shell (composition: *Fe* with 0.003% *C*, 0.08% *Mn*, 0.005% *Si*, 0.015% *P*, 0.01% *S*, 0.01% *Cr*, 0.01% *Ni*, 0.01% *Cu*, 0.05% *Ti*, and 0.04% *Al*), as it moves down the 230-mm thick parallel mold at a casting speed (*v*) of 23.33 mm/s or 1.4 m/min. The liquidus and solidus temperatures of this steel grade are 1533 $^{\circ}$C and 1517 $^{\circ}$C, respectively. The mold oscillation frequency and stroke are 2.58 Hz or 155 cpm and 6.34 mm, respectively. These casting parameters correspond to typical operating practice in the steel industry, such as POSCO, South Korea [2, 5]. Figure 2(a) shows the computational domain, which is a 3 mm x 30 mm longitudinal slice along the centerline of the wide face (1300-mm in length) near the meniscus.
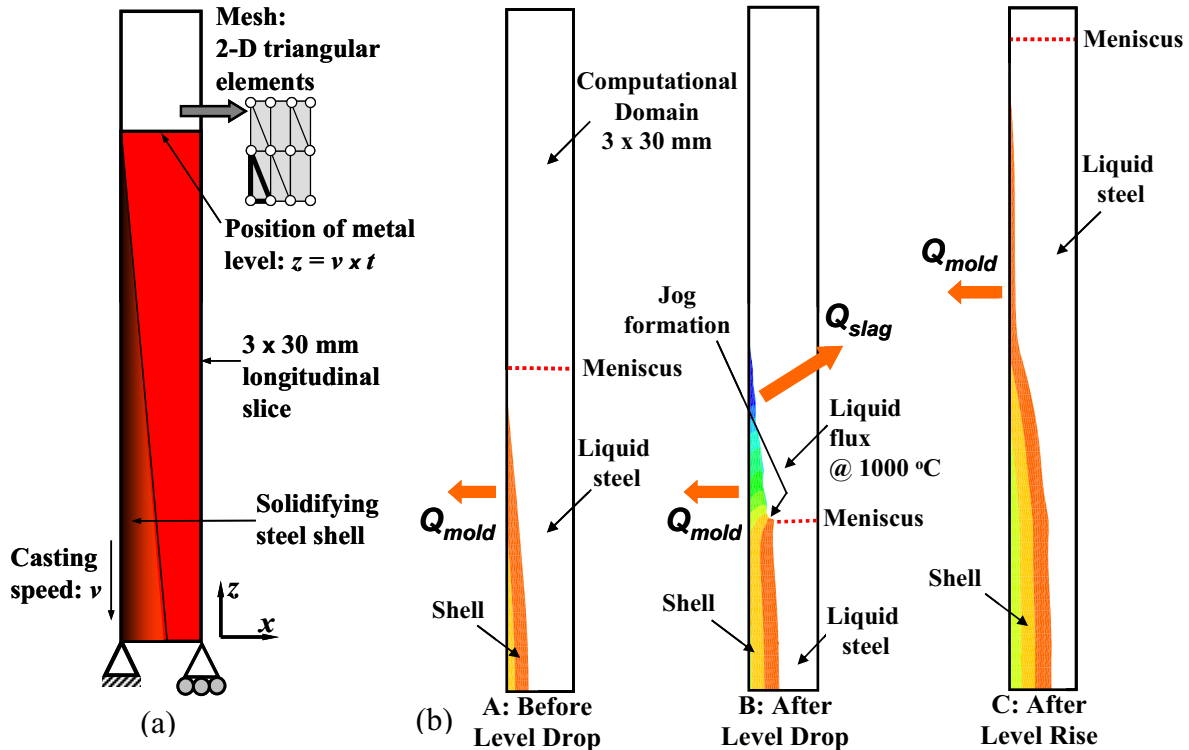

Figure 2: (a) Computational domain and mechanical boundary conditions used in CON2D for predicting shell distortion due to a sudden level fluctuation event during the casting process, and (b) thermal boundary conditions for the three different stages of the event.

The longitudinal slice enters the mold and moves downwards at the casting speed. Solidification proceeds from the left edge of the domain. At any time *t*, the metal level (ignoring meniscus curvature) is located just above the shell tip at $z = v \times t$ mm (see Figure 2(a)). Then, a sudden drop in metal level (by Δh mm) at $t_{drop} = 0.69$ s is imposed, exposing the inner edge of the shell to the liquid flux layer that floats above the liquid steel. Finally, a subsequent level rise occurs at $t_{rise} = 1.09$ s. The duration of the level fluctuation, $\Delta t = 0.4$ s corresponds to an oscillation cycle, or a chaotic wave generated by the turbulent flow. Figures 3(a) and (b) track the metal level changes in moving and stationary frames of reference, respectively, which are used to simulate a single level fluctuation event.

The heat flow model solves the 2-D transient energy equation, using a fixed Lagrangian grid of 3-node triangles. Temperature-dependent thermal conductivity and enthalpy functions are used to incorporate the effects of solidification and solid-state phase transformation on the heat flow across the domain [19]. A non-equilibrium micro-segregation model incorporating the effects of several alloying elements is used to calculate the liquidus, solidus, and peritectic temperatures,

and phase fractions [20]. Within each time step, temperatures are first computed by the heat transfer model. After interpolating the thermal loads onto a fixed-grid finite element mesh of 6-node triangles, the stress model then solves for stresses, strains, and displacements. The effects of stiffness and volume changes during solidification are incorporated through temperature-dependent Young's modulus and thermal linear expansion functions [19].
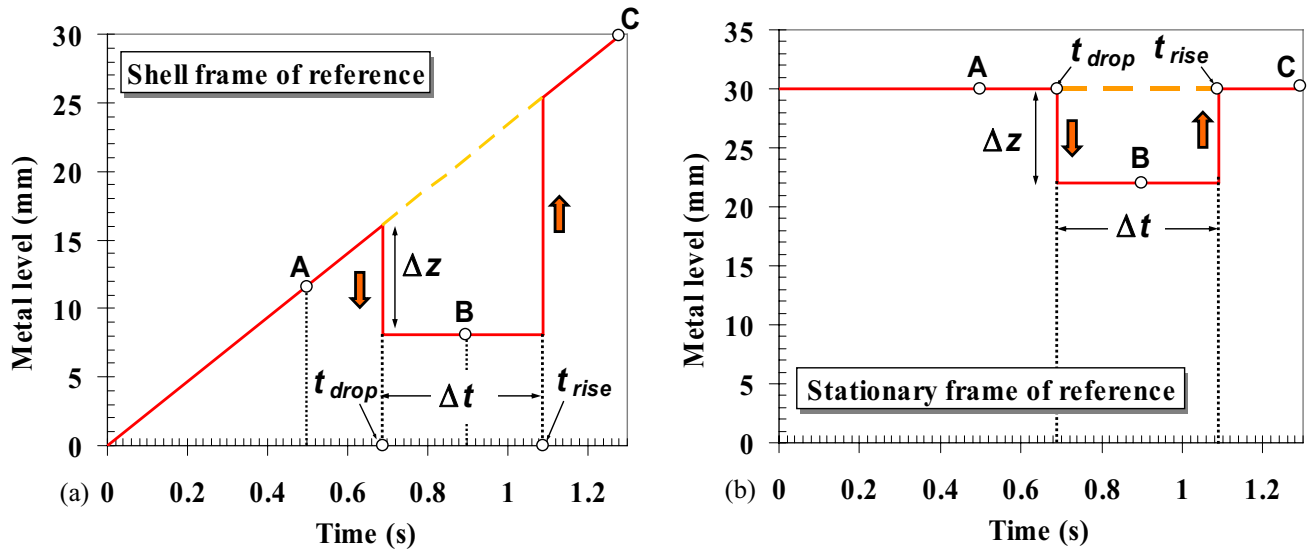

Figure 3: Position of metal level inside the computation domain during a level fluctuation event in the (a) moving (attached to shell) and (b) stationary frames of reference. A, B, and C are three specific instants during the level fluctuation event – *i.e.* before level drop, after level drop, and after level rise, respectively. *Legend:* —— *with &* – – *without level fluctuation.*

To discretize the computational domain, a grid size of 31 nodes x 61 nodes (mesh resolution: 0.1 mm x 0.5 mm) was selected based on a sensitivity analysis conducted for a normal solidification case without any level fluctuation. The results in Figure 4 show that increasing the number of nodes either in the *x* or *z* directions does not change the model predictions (*e.g.* axial stress, σ_{zz}). The effectiveness of handling the liquid elements is seen in Figure 4(a), by the suppression of stress above the solidus temperature. Figure 4(b) also indicates that tensile stresses are generated near the solidification front and at the slab surface, which subsequently switches to compression due to the volumetric changes associated with $\delta \rightarrow \gamma$ transformation.

The computational domain is initially assumed to contain stress free liquid at a uniform temperature, corresponding to a pour temperature of 1565 $^{\circ}$C employed during the casting process. Solidification within the domain is achieved by imposing a Cauchy-type heat transfer boundary condition on the left edge corresponding to the heat flow towards the water-cooled mold. However, zero heat flux boundary condition is imposed on a portion of the left edge located above the metal level.

The heat flux (Q_{mold} in W/m^2) boundary condition corresponding to mold (or primary) cooling before the level drop (event "A" in Figure 2(b)) is given by:

$$Q_{mold} = 0 \qquad\qquad \text{for } t > 0 \text{ s, } x = 0 \text{ mm, } \& \ z > z = v \times t \qquad\qquad (1)$$
$$Q_{mold} = h_{mold} (T - T_{mold}) \qquad \text{for } t > 0 \text{ s, } x = 0 \text{ mm, } \& \ z \leq z = v \times t \qquad\qquad (2)$$

The mold wall is assumed to be at a constant (sink) temperature of T_{mold} = 250 $^{\circ}$C, and the heat transfer coefficient, h_{mold} of 4000 W/m^2-K (corresponding to a heat flux of ~5.0 MW/m^2 near the

meniscus) is used in the heat flow model. Zero heat flux is assumed across the top, bottom, and the liquid steel sides of the domain.

At time, t_{drop} = 0.69 s, the level drops suddenly by ~16 mm (event "B" in Figure 2(b)) for a duration of 0.4 s. During this time, the thermal conductivity and specific heat of the nodes in the liquid steel region (beyond the solidification front) are artificially lowered to simulate the entrance of liquid flux at a constant temperature of T_{flux} = 1000 °C in the domain to replace the liquid steel. The following boundary condition is imposed along the exposed solid shell, defined by the location of the solidus isotherm at the time of the level drop:

$$Q_{flux} = h_{flux} (T - T_{flux}) \qquad \text{for } t_{drop} \leq t \leq t_{rise} \text{ with } h_{flux} = 1500 \text{ W/m}^2\text{-K} \qquad (3)$$
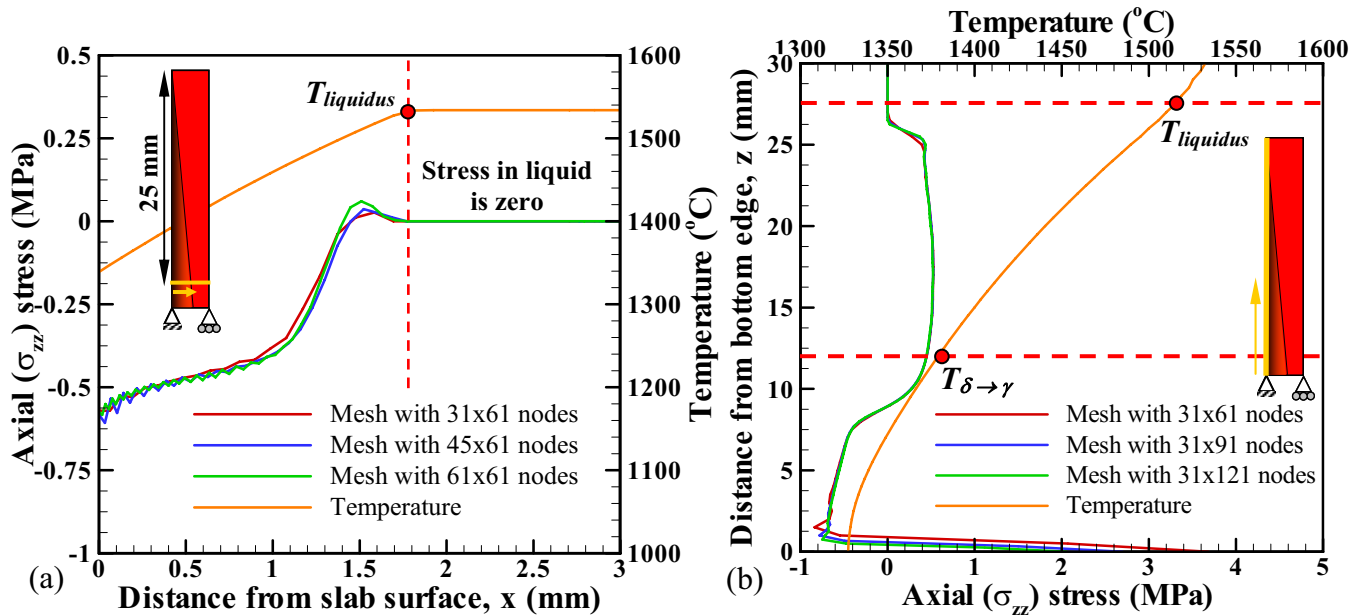

Figure 4: Axial stress (σ_{zz}) for 3 different mesh sizes (a) across shell at 25 mm below the shell tip (increasing nodes in x-direction), and (b) along shell surface (increasing nodes in z-direction).

Finally, the level is raised again at time, t_{rise} = 1.09 s (event "C" in Figure 2(b)), by restoring the liquid elements at the initial temperature, and allowing solidification to proceed normally. Since the level is restored above the shell tip, the model simulates meniscus overflow, which is an important event associated with oscillation mark formation [9, 10, 17, 18]. The model ignores non-uniform dissipation of superheat and nucleation under-cooling near the meniscus, hence the possibility of meniscus solidification is not considered.

The mechanical boundary conditions imposed on the domain are indicated in Figure 2(a). The shell tip is free to move away or towards the mold so that the formation of an oscillation mark or a surface depression can be simulated. Rigid body motion in the domain is prevented by fixing three nodal displacements of the bottom-left node and by preventing the movement of the bottom edge along the casting direction. Mold friction and pressure forces imposed on the shell by the liquid flux and slag rim (~1 kPa), and ferrostatic pressure (~0.002 MPa at the bottom of the domain) are ignored. Although these effects are important to meniscus shape, they are not expected to affect the distortion of the solid shell caused by thermal stress, which is in the range of ± 1.0 MPa, as indicated in Figure 4. The longitudinal slice is assumed to remain planar as it moves down the mold; thus, the stress state in the wide and thin shell follows a generalized plane strain mode, allowing the 2-D model to reasonably estimate a complete 3-D stress state for the domain under consideration.

Results and Discussions

Figure 5 shows the evolution of shell shape and distortion at three different times during the level fluctuation event (refer to Figure 3) computed by the model as the domain traverses the mold length consistent with the casting speed. Figures 6(a) and (b) show the distribution of temperature and axial stress (σ_{zz}), respectively, at these instants across the shell thickness and along a line 5 mm above the bottom edge of the domain. The stresses across the thickness (σ_{xx}) and in the transverse direction (σ_{yy}) are very small ($< \pm 1.0$ MPa) for a shell length of ~16 mm owing to rapid creep relaxation and low elastic modulus at high temperatures. Referring to these figures, it can be seen that before the level drop event, solidification dictated by heat flow towards the mold proceeds with time and a thermal gradient quickly develops inside the shell. The surface cools rapidly, causing the shell tip to bend towards the mold (by ~0.02 mm) and axial tensile stress to develop near the surface.

After the level drops, exposing the shell to mold flux, the shell temperature decreases rapidly (~200 ^{o}C in 0.19 s) because the mold extracts sensible heat from the thin shell very quickly in the absence of heat supply from the liquid steel. The thermal gradient inside the shell also disappears, causing the shell interior to contract more than its exterior. Thus, a relatively large compressive stress develops at the surface, and the shell tip bends away from the mold wall (by ~0.04 mm). Suddenly raising the liquid level back up to the shell tip, is predicted to rapidly increase the shell temperature, shell thickness, and distortion. Liquid steel comes in direct contact with the colder shell, and a new skin grows over the older shell. Restoring the high temperature gradient across the entire thickness tends to cause the older shell to expand. Because this is constrained by the newly-solidified layer, the net effect is to bend the shell tip substantially towards the liquid steel, (up to 0.46 mm within 0.21 s time span).

Although a level drop of ~16 mm was chosen in the previous case to demonstrate the thermo-mechanical behavior of the shell during a level fluctuation event, a level drop of this magnitude occurs only rarely in an industrial casting machine, and is normally within ±10 mm [21]. Thus, the model was utilized to compute the shell shapes and distortions for smaller level fluctuations keeping the duration constant at 0.4 s. The results are summarized in Figure 7(a), which indicates that shell tip distortion is almost negligible for fluctuations below ~5 mm.

An irregularity in the profile of the inner shell edge was always observed near the location where the liquid level stays stationary for 0.4 s during the level drop event. Ordinary solidification below this location increases the shell thickness, in contrast to the shell edge above this location, which does not grow due to the absence of liquid steel. Thus, the formation of a "jog" (refer to Figure 2(b)) is predicted by the model, similar to the one observed in the plant sample in Figure 7(b). This jog is smoothened out after the liquid level rise.

The thermally distorted shell shape predicted for a level drop of ~16 mm is compared in Figure 8(a) with actual hook shapes (*i.e.* traces of lines of hook origin) from specially-etched micrographs [4, 6], which were obtained from a 230 mm x 1300 mm ultra-low carbon steel slab cast at POSCO [5] under similar casting conditions. Figure 8(a), also shows the shape of the liquid steel meniscus calculated by Bikerman's equation [22]. All of the hooks are curved much more than the maximum curvature expected from thermal distortion of the initial shell, even for a large level fluctuation of 16 mm for 0.4 s. Furthermore, the measured shapes match reasonably well with the predicted meniscus shape. This suggests that the formation of curved hooks is indeed a meniscus freezing-controlled event. However, the figure also suggests that the bottom portion of the straight hooks (located close to the surface) may be formed by the thermal distortion effect after level fluctuations.
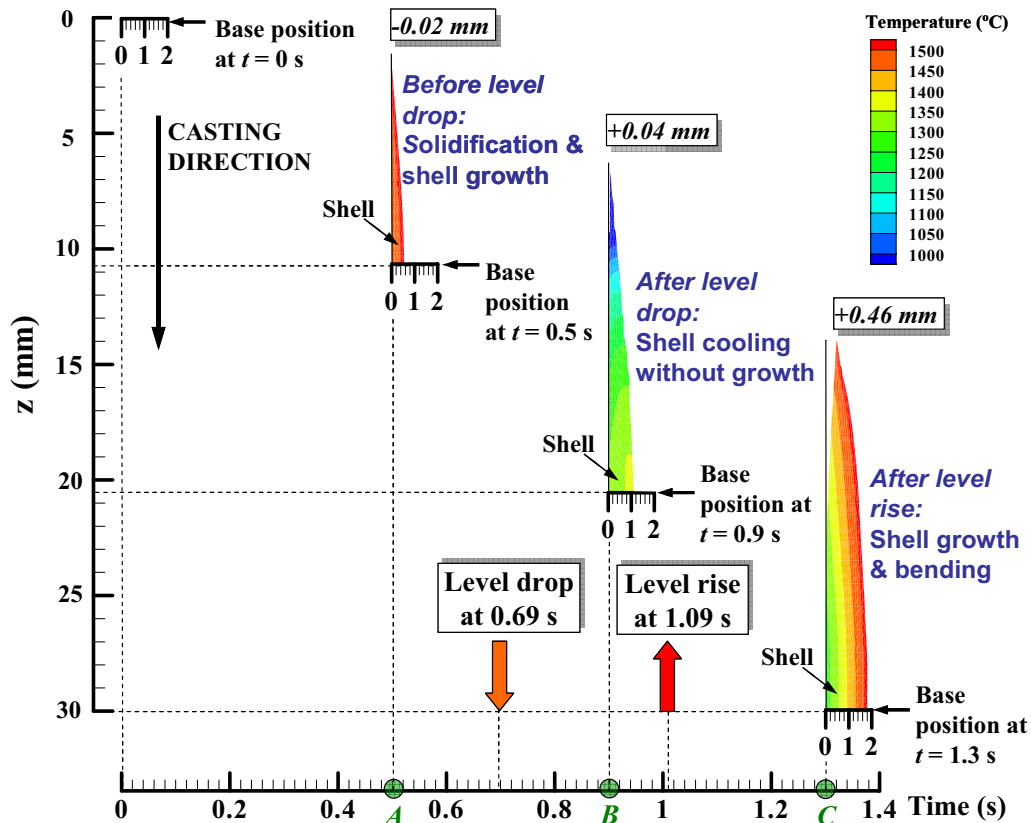
Figure 5: Evolution of temperature field and shell tip deformation during a level fluctuation event. Plots for three representative times are shown: (A) 0.19 s before the level drops, (B) 0.21 s after the level drops, and (C) 0.21 s after the level rises again (meniscus overflow).
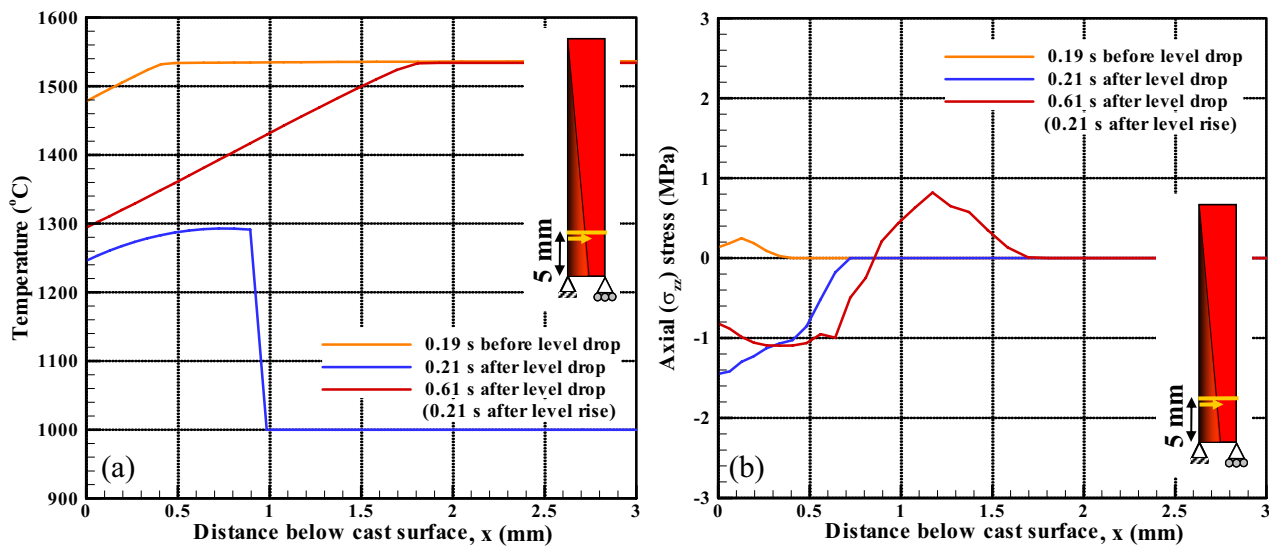

Figure 6: (a) Temperature and (b) Axial stress (σ_{zz}) profiles through the shell (5 mm above the bottom edge) during the level fluctuation event.

Based on this proposition, Figure 8(c) schematically presents a tentative mechanism for straight hook (such as one shown in Figure 8(b) with a hook depth of 0.48 mm) and oscillation mark formation. Assuming that level fluctuations periodically occur during every mold oscillation cycle, the steps in formation of hooks and oscillation marks in ultra low carbon steel are as follows:

(i) At the start of the negative strip period, the metal level drops causing the shell tip to bend away from the mold wall. The shape of the shell edge facing the mold at this instant dictates the curvature of the line of hook origin.

(ii) The metal level rises and overflows over the line of hook origin.

(iii) The overflowed liquid solidifies. Until this happens, the extent of the penetration of this liquid into filling the gap and re-melting the interfacial flux layer determines the final shape of the upper side of the oscillation mark.

(iv) Any debris trapped within the overflowed liquid creates surface defects.

(vii) The hook protruding from the solidifying shell captures inclusions/bubbles rising up the solidification until the shell finally solidifies past the hook.
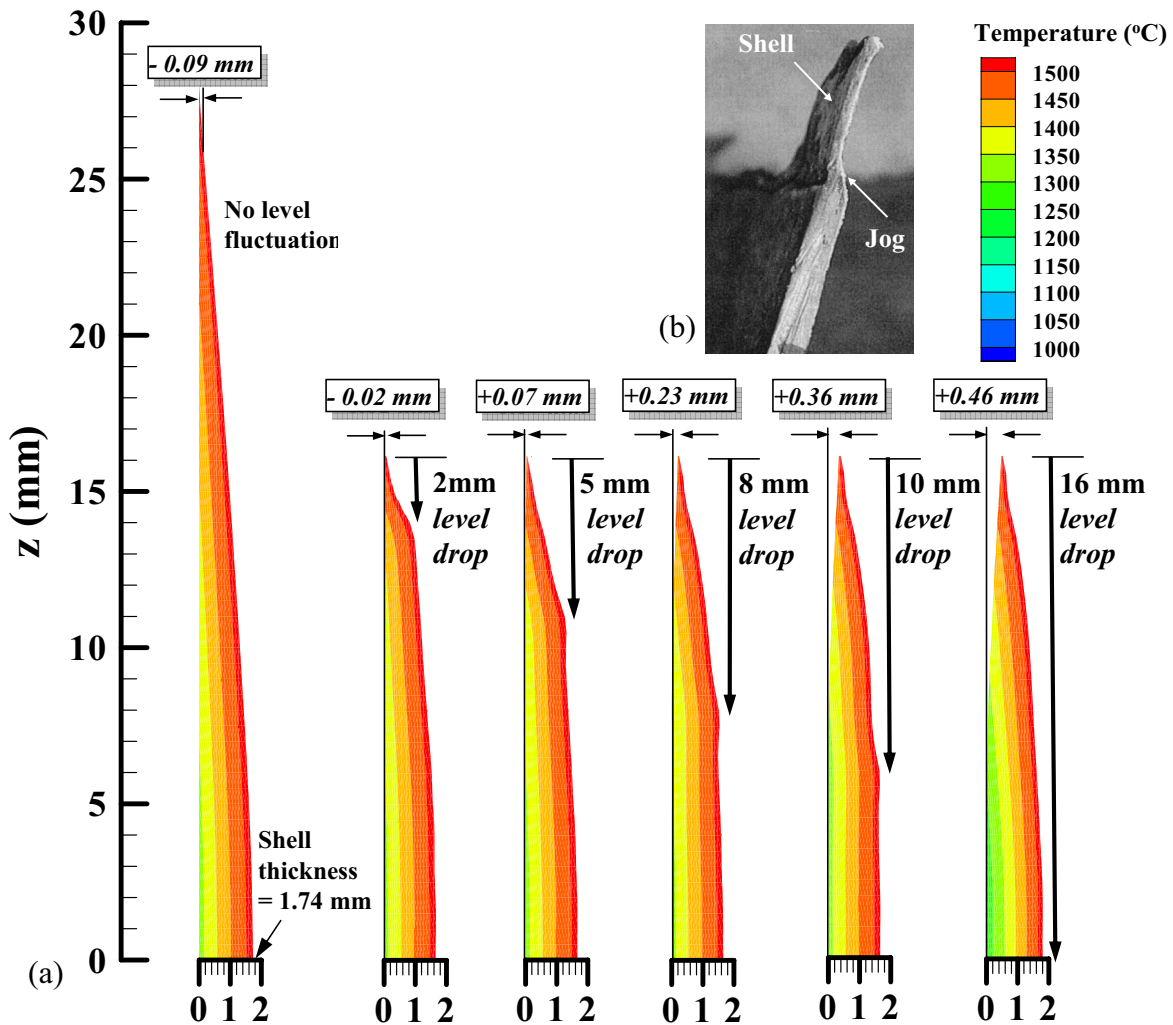

Figure 7: (a) Comparison between shell distortion predictions for different magnitudes of level drop and normal solidification (no level fluctuation). (b) Jog formation on the inside edge of the shell observed by Fredriksson and Elsberg [23] in a breakout shell.

Conclusions

A 2-D transient FE model has been successfully used to reasonably predict shell shape and distortion due to a sudden level fluctuation event for ultra-low carbon steel slabs. A sudden level drop causes the shell tip to bend away from the mold. Subsequent rise in liquid level causes further shell bending. Shell distortion can be ignored for rapid level drops less than ±5 mm; however, for larger drops, such as 16 mm for 0.4 s, shell bending can be up to 0.46 mm for a 16 mm long shell. Although shell distortion alone cannot produce curved hooks and their associated oscillation marks, there is a possibility that shallower straight hooks can be created by this

mechanism. In particular, ultra-low carbon steels and peritectic steels, which tend to produce a stronger initial shell that cannot be flattened by ferrostatic pressure, can be expected to suffer from thermal distortion effect.
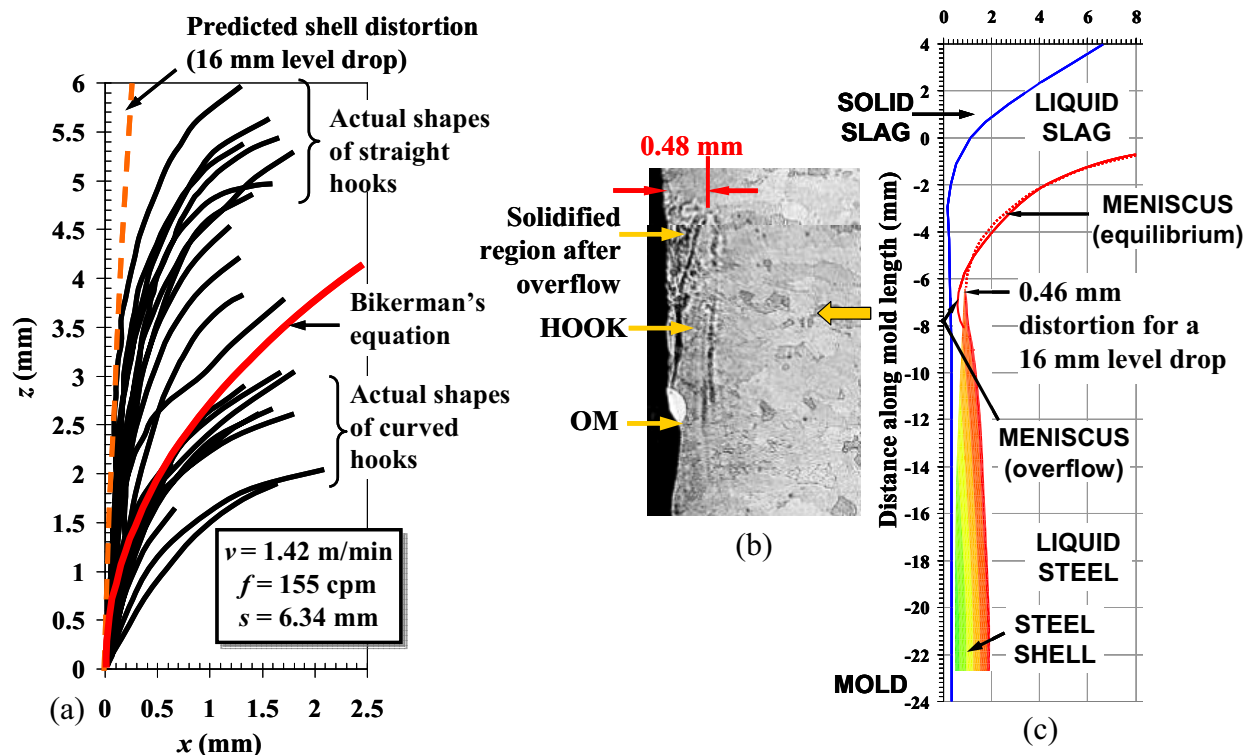

Figure 8: (a) Comparison of actual and predicted hook shapes, (b) actual straight hook, and (c) shell distortion and meniscus overflow-based hook formation mechanism for straight hooks.

Acknowledgements

References

1. K. D. Schmidt et al., "Consequent improvement of surface quality by systematic analysis of slabs", *Steel Research International*, 74(11-12) (2003), 659-666.
2. H.-J. Shin et al., *MS&T 2004 Conference Proceedings*, (The Association for Iron and Steel Technology (AIST) and TMS, Warrendale, PA, 2004), 11-26.
3. M. Suzuki, "Initial solidification behaviour of ultra low carbon steel", *CAMP-ISIJ*, 11 (1998), 42-44.
4. J. Sengupta et al., "Micrograph evidence of meniscus solidification and sub-surface microstructure evolution in continuous-cast ultra-low carbon steels", (forthcoming in Acta Materialia, 2005).
5. H.-J. Shin et al., *AISTech 2004 Iron & Steel Technology Conference Proceedings - Vol. II*, (The Association for Iron & Steel Technology (AIST), Warrendale, PA, 2004), 1157-1170.
6. J. Sengupta et al., "A new mechanism of hook formation during continuous casting of ultra-low carbon steel slabs", (accepted in Metallurgical & Materials Transactions A, 2005).

7. C. Genzano et al., "Elimination of surface defects in cold-rolled extra low carbon steel sheet", *Iron and Steel Maker*, 29(6) (2002), 23-26.

8. G.-G. Li, and S.-H. Kim, private communication with authors, Department of Materials Science & Engineering, Pohang University of Science & Technology (POSTECH), South Korea, Spetember, 2004.

9. T. Emi et al., "Influence of physical and chemical properties of mold powders on the solidification and occurrence of surface defects of strand cast slabs", *Proceedings of National Open Hearth and Basic Oxygen Steel Conference*, 61 (1978), 350-361.

10. K. Schwerdtfeger, and H. Sha, "Depth of oscillation marks forming in continuous casting of steel", *Metallurgical and Materials Transactions B*, 31B (2000), 813-826.

11. I. G. Saucedo, *Steelmaking Conference Proceedings*, (ISS-AIME, Warrendale, PA, 1991), 43-53.

12. E. Takeuchi, and J. K. Brimacombe, "Effect of oscillation-mark formation on the surface quality of continuously cast steel slabs", *Metallurgical Transactions B*, 16B (1985), 605-625.

13. H. Yamamura et al., "Formation of solidified hook-like structure at the subsurface in ultra low carbon steel", *ISIJ International (Supplement)*, 36 (1996), S223-226.

14. E. S. Szekeres, "Overview of mold oscillation in continuous casting", *Iron and Steel Engineer*, 73(7) (1996), 29-37.

15. R. Sato, *Proceedings of National Open Hearth and Basic Oxygen Steel Conference*, (AIME, Warrendale, PA, 1979), 48-67.

16. J. Savage, and W. H. Pritchard, "Problem of rupture of billet in continuous casting of steel", *Iron and Steel*, 27(14) (1954), 649-652.

17. J. L. Brendzy et al., "Mould-strand interaction in continuous casting of steel billets: Part 2. Lubrication and oscillation mark formation", *Ironmaking and Steelmaking*, 20 (1) (1993), 63-74.

18. B. G. Thomas, and H. Zhu, *Proceedings of JIM/TMS Solidification Science and Processing Conference*, (TMS, Warrendale, PA, 1995), 197-208.

19. C. Li, "Thermal-mechanical model of solidifying steel shell behavior and its applications in high speed continuous casting of billets" (Ph. D. Thesis, University of Illinois at Urbana-Champaign, Urbana IL, 2004).

20. Y. Meng, and B. G. Thomas, *Metallurgical Transactions B*, 34B (2003), 685-705.

21. W. Lai et al., *83rd Steelmaking Conference Proceedings*, (ISS-AIME, Warrendale, PA, 2000), 261-274.

22. I. Jimbo, and A. W. Cramb, "Calculations of the effect of chemistry and geometry on free surface curvature during casting of steels", *Iron & Steelmaker*, 20(6) (1993), 55-63.

23. H. Fredriksson, and J. Elfsberg, "Thoughts about the initial solidification process during continuous casting of steel", *Scandinavian Journal of Metallurgy*, 31 (2002), 292-297.